

International Conference on Space Optics—ICSO 2022

Dubrovnik, Croatia

3–7 October 2022

Edited by Kyriaki Minoglou, Nikos Karafolas, and Bruno Cugny,



Out-of-focus point sources image simulation for the Metis solar coronagraph onboard the Solar Orbiter mission



Out-of-focus point sources image simulation for the Metis solar coronagraph onboard the Solar Orbiter mission

Vania Da Deppo^{*a,b}, Chiara Casini^{a,b,c}, Paolo Chioetto^{a,b,c}, Fabio Frassetto^{a,d}, Simone Nordera^{a,b}, Paola Zuppella^{a,b}, Alain J. Corso^a, Federico Landini^d, Maurizio Pancrazzi^d, Roberto Susino^d, Clementina Sasso^e, Michela Uslenghi^f, Marco Romoli^g, Vincenzo Andretta^e, Silvano Fineschi^d, Giampiero Naletto^{h,a,b,c}, Gianalfredo Nicolini^d, Daniele Spadaroⁱ, Marco Stangalini^j, Luca Teriaca^k, Lucia Abbo^d, Catia Grimani^{l,m}, Aleksandr Burtovoiⁿ, Yara De Leo^{k,o}, Michele Fabi^l, Federica Frassati^d, Giovanna Jerse^p, Giuliana Russano^e

^aCNR-Istituto di Fotonica e Nanotecnologie, Padova, Via Trasea 7, 35131 Padova, Italy; ^bINAF-Osservatorio Astronomico di Padova, Vicolo dell'Osservatorio 5, 35122 Padova, Italy; ^cCISAS Centro Interdipartimentale Studi e Attività Spaziali “G. Colombo”, Via Venezia 15, 35131 Padova, Italy; ^dINAF-Osservatorio Astrofisico di Torino, Strada Osservatorio 20, 10025 Pino Torinese (TO), Italy; ^eINAF-Osservatorio Astronomico di Capodimonte, Salita Moiariello 16, 80131 Napoli, Italy; ^fINAF-Istituto di Astrofisica Spaziale e Fisica cosmica, Via Alfonso Corti 12, 20133 Milano, Italy; ^gDipartimento di Fisica ed Astronomia - Università degli Studi di Firenze, Via G. Sansone 1, 50019 Sesto Fiorentino (FI), Italy; ^hDipartimento di Fisica e Astronomia “Galileo Galilei” - Università degli Studi di Padova, Via Marzolo 8, 35131 Padova, Italy; ⁱINAF-Osservatorio Astrofisico di Catania, Via S. Sofia 78, 95123 Catania, Italy; ^jASI, Via del Politecnico, 00133 Roma, Italy; ^kMax Planck Institute for Solar System Research, Justus-von-Liebig-Weg 3, 37077 Göttingen, Germany; ^lUniversità degli Studi di Urbino Carlo Bo, Via S. Chiara 27, 61029 Urbino (PU), Italy; ^mINFN Sezione di Firenze, Via G. Sansone 1, 50019 Sesto Fiorentino (FI), Italy; ⁿINAF – Osservatorio Astrofisico di Arcetri, Largo Enrico Fermi 5, 50125 Firenze, Italy; ^oDip. di Fisica e Astronomia, Università di Catania, Piazza Università 2, 95131 Catania, Italy; ^pINAF-Osservatorio Astronomico di Trieste, Via Giambattista Tiepolo 11, 34143 Trieste, Italy

ABSTRACT

Metis is a multi-wavelength coronagraph onboard the European Space Agency (ESA) Solar Orbiter mission. Thanks to the selected Solar Orbiter mission profile, for the first time the poles of the Sun and the circumsolar region will be seen and studied from a privileged point of view near the Sun (minimum distance 0.28 AU).

Metis features an innovative instrument design conceived for simultaneously imaging the visible (580-640 nm) and ultraviolet (Lyman α at 121.6 nm) emission of the solar corona. METIS is an externally occulted coronagraph which adopts an “inverted occulted” configuration. The inverted external occulter (IEO) is a circular aperture after which a spherical mirror M0 rejects back the solar disk light, which exits the instrument through the IEO aperture itself. The passing coronal light is then collected by the METIS telescope. Common to both channels, the Gregorian on-axis telescope is centrally occulted and both the primary and the secondary mirrors have annular shape.

The optical and radiometric performance of the telescope is strongly dependent on the huge degree of vignetting presented by the optical design. The internal fields are highly vignetted by M0 and further vignetted by the internal elements, such as the internal occulter and the Lyot stop, furthermore the presence of some spiders, needed to mount the internal elements, are vignetting even more, in some parts of the FoV, the light beams.

*vania.dadeppo@ifn.cnr.it; phone +39-049 9815639

During the instrument commissioning, in the visible light channel some out-of-focus sources have been imaged while moving in the Metis FoV. At a first glance, the out-of-focus images exhibit a very strange pattern. The pattern can be explained by taking into account the peculiar design of the Metis coronagraph instrument; in fact, the not fully illuminated pupil gives rise to “half moon” shape out-of-focus images with the spiders casting their shadow in different positions. In this work, the ray-tracing simulation results for the out-of-focus images are compared with some of the images taken in flight; some considerations relating the shape and dimension of the acquired images with the distance from Metis of the sources are also given.

Keywords: Metis coronagraph, Solar Orbiter mission, optical simulation, out-of-focus images

1. INTRODUCTION

Solar Orbiter (SO) is a mission dedicated to study solar and heliospheric physics[1]. SO is the first medium-class mission of ESA’s Cosmic Vision 2015-2025 Programme and has been developed in collaboration with NASA. With a combination of in-situ and remote sensing instruments, SO is conceived for the circumsolar region exploration to give an answer to the scientific questions on how the heliosphere is generated and controlled by the Sun.

Launched in February 2020, the mission will provide close-up, high-latitude observations of the Sun. SO will have a highly elliptic orbit (0.9 AU at aphelion and 0.28 AU at perihelion). Thanks to its mission profile, for the first time the poles of the Sun and the circumsolar region will be seen and studied from a privileged point of view near the Sun.

Soon after launch, SO underwent the Near Earth Commissioning Phase (NECP), the spacecraft and the payload were functionally checked and calibrated. Also the Metis coronagraph [2], which is one of the remote sensing instruments mounted on board the SO spacecraft, was switched on, functionally tested and characterized [3]. In particular, the two mechanisms of the instrument, the one-shot sealing cap and the internal occulter mechanism (IOM), were activated.

The Metis instrument is conceived to image the solar corona in two different spectral bands: the UV narrow band HI Lyman- α at 121.6 nm, and the polarized broad-band visible light (580 – 640 nm). The instrument is designed to image the structure and dynamics of the full corona in the range from 1.6 to 3.1 solar radii (R_s), at minimum perihelion distance (0.28 AU), and from 2.8 R_s to 5.5 R_s , at 0.5 AU.

In this paper, after a description of the Metis optical design, the ray-tracing simulations for out-of-focus objects are presented and discussed and compared with some images taken in flight during the commissioning phase.

2. METIS OPTICAL DESIGN AND VIGNETTING FUNCTION

2.1 Metis optical design

Metis adopts an “inverted externally occulted” configuration (see Figure 1) [4], which allows the thermal loads inside the instrument to be reduced. The inverted external occulter (IEO), a small aperture on the spacecraft thermal shield, also acts as the entrance pupil of the instrument. The solar disk light entering the Metis aperture is stopped and back-reflected outside the instrument by a spherical mirror (M0) [5].

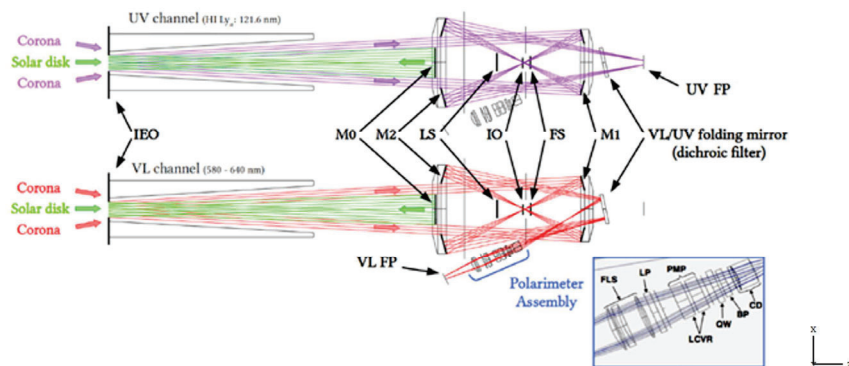


Figure 1. Metis layout. The raytraces of the two channels are depicted separately. On the top the UV channel and on the bottom the VL one with a zoom on the VL polarimeter assembly.

The Metis telescope is then collecting the passing coronal light. The Gregorian on-axis Metis telescope is centrally occulted and both the primary and the secondary mirrors have annular shape [6].

The primary mirror (M1) focuses the gathered coronal light in its focal plane. Here a field stop (FS) is placed and limits the outer FOV of the coronagraph. Then the secondary mirror (M2) focalizes the light again; part of the light (UV Ly- α) passes through the interference filter (IF) and hence is collected by UV detector; the other part, mostly visible, is reflected by the IF and is directed to the polarimeter assembly.

Stray light minimization is a mandatory goal in any coronagraph and the worst offenders are the surfaces hit by the direct solar disk light, IEO and M0. The internal occulter (IO) and the Lyot stop (LS) are, respectively, conjugated with the IEO and M0 via the primary mirror M1. IO blocks the solar disk light diffracted by the IEO edge, while LS blocks the light diffracted by the M0 edge [7] [8].

In summary, Metis consists of a single optical head that incorporates two different channels: a UV imaging channel and a polarimeter visible light (VL) channel. The telescope optics (M1 and M2) and the stop system (IEO, M0, FS, IO and LS) are common to both channels, while the VL channel has a dedicated relay optics and a polarizing group. Each channel has its own detector respectively called UVDA and VLDA.

The annular Field of View (FoV) covered by the Metis instrument is between 1.6° and 2.9°, and the attained spatial resolution is 20". Along the diagonals of the field, a 3.4° field angle is reached. As for the inner telescope field angles, till about 1.5°, the light is not transmitted since the light beams are completely blocked by the M0 mirror. For the other fields, the light is partly vignetted by M0 and then by the other internal stops, i.e. FS, IO, and LS.

The Metis instrument optical specifications are summarized in Table 1.

Table 1 Summary of Metis instrument optical characteristics.

<u>Metis instrument optical specifications</u>	
FoV	1.6°-2.9° (1.6°-3.4° along the diagonal) 1.7-3.1 R _s @ 0.28 AU – 3.0-5.5 R _s @ 0.5 AU
Telescope type	Externally occulted on-axis Gregorian
Effective focal length	VL: 200 mm UV: 300 mm
Wavelength range	VL: 580-640 nm UV: 121.6 ± 10 nm
Spatial resolution	VL: < 20 arcsec @ > 2° < 40 arcsec @ < 2° UV: < 20 arcsec
Average Straylight (B _{cor} /B _{sun})	VL < 10 ⁻⁹ UV < 10 ⁻⁷
Detectors	VL: 2048x2048 10 μm pixel size UV: 1024x1024 15 μm pixel size (eq. 30 μm)

2.2 Metis vignetting function

An important characteristic of the Metis coronagraph is its vignetting function ([9][10]). As already mentioned, the light passing through the Metis telescope body is highly vignetted by M0 and then furtherly vignetted by IO and LS. Moreover, on the diagonals of the image, the two four-spider systems supporting respectively the M0/LS assembly and the IO/FS assembly are vignetting the beam even more. In Figure 2(a), the whole opto-mechanical layout of Metis is presented and in the bottom right part of the picture the two IO/FS and M0/LS assemblies with the supporting spiders are shown. The internal occulter mechanism, with the four-spider system clearly visible, is shown in Figure 2(b).

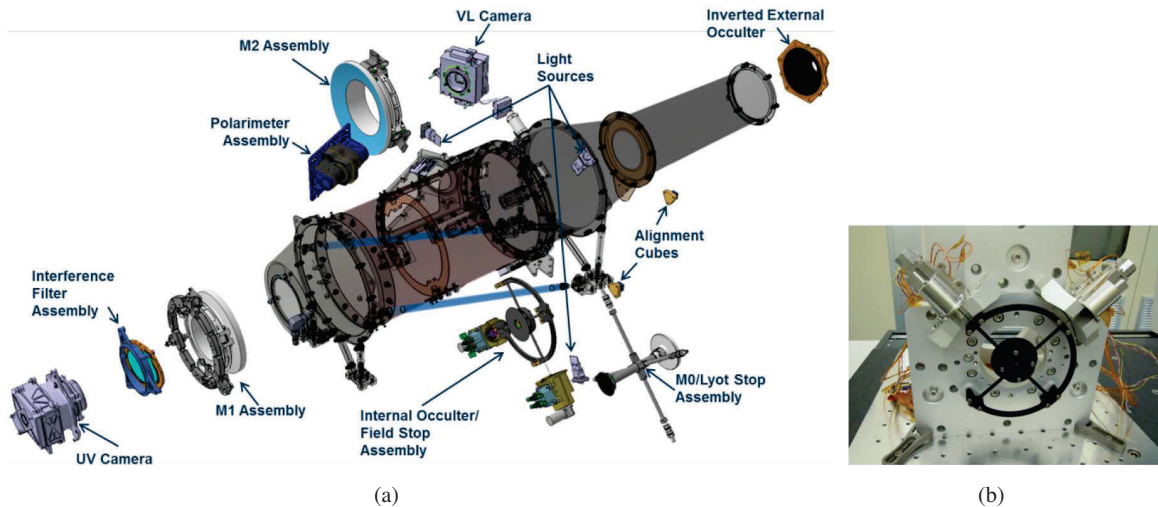


Figure 2. In (a) opto-mechanical subsystems of Metis. In (b) picture of the flight model of the internal occulter mechanism with the four-spider system painted in black clearly visible [2].

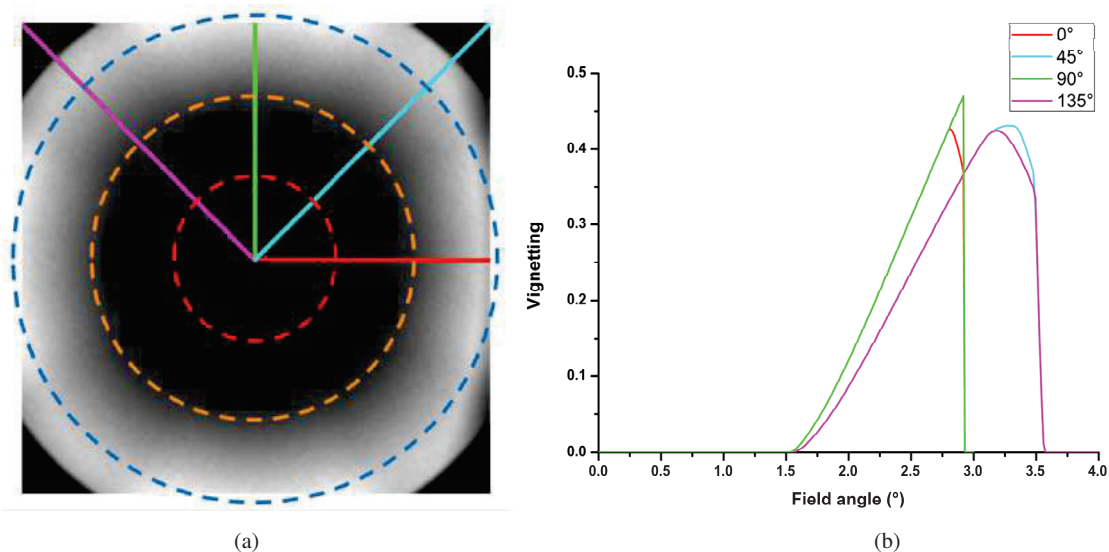


Figure 3. Dependence of the Metis vignetting function on the radial field of view. (a): Gray scale representation of the bidimensional vignetting function, as obtained by ray-tracing; overlapped dashed circles represent 1° (red), 2° (orange), and 3° (blue) FoVs. (b): plots of the vignetting function along the radial directions shown in (a) as a function of the different colours.

Over the nominal FoV of the telescope the fraction of unvignetted rays is always less than 50%. See Figure 3 for the Metis theoretical vignetting function given both in terms of 2D image in (a) and as radial profiles in (b). The further vignetting due to the spiders is clearly visible by comparing the profiles at 0° and 90° with the 45° and 135° ones.

3. OUT-OF-FOCUS IMAGES AND SIMULATIONS

On the 10th of February 2020 (04:03 UTC), the Solar Orbiter spacecraft has been launched by an Atlas V rocket from Cape Canaveral. Soon after launch, the switch on and commissioning of the payload instruments started. During the commissioning [3], in particular in June 2020 some sessions foreseen for the straylight measurements and internal occulter adjustment after launch have taken place [8]. During one of these sessions, in the visible channel of Metis unexpectedly

appeared a series of out-of-focus peculiar images (see Figure 4). This fact triggered the Metis team curiosity in trying to understand in which way these strange images are generated.

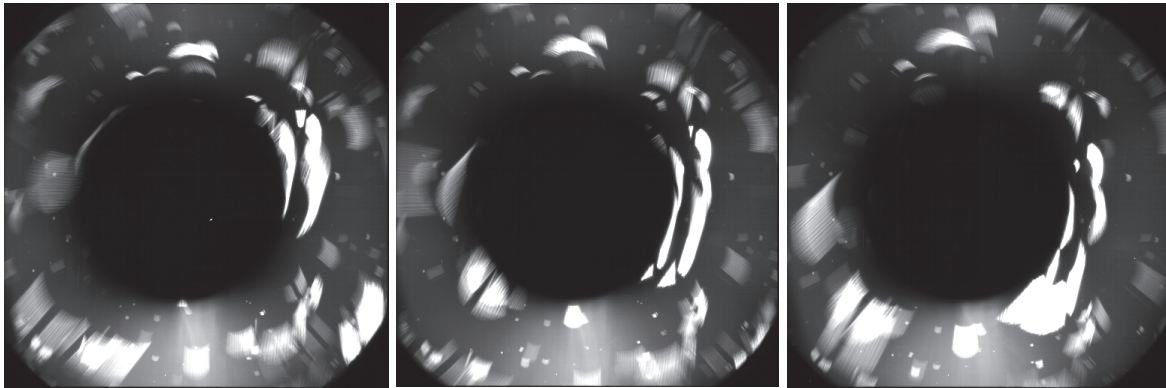


Figure 4. Series of frames taken with Metis in June 2020 with peculiar out-of-focus patterns.

3.1 Out-of-focus images seen with other coronagraphs

Occasionally, bright blobs or streaks have already been seen appearing in images taken with space coronagraphs, e.g. COR instruments [11] onboard STEREO and LASCO [12][13] onboard SOHO, see Figure 5. These features are likely to be generated by small pieces of the multi-layer thermal insulation (MLI) blankets that are moving around in the instrument FoV. The MLI is wrapped around the spacecraft and micrometeorite impacts could knock off small MLI pieces and generate a sort of small particle shower. As for the narrow streaks, generated by sources farther away from the spacecraft, potentially they could also be interplanetary, or cometary, dust grains.

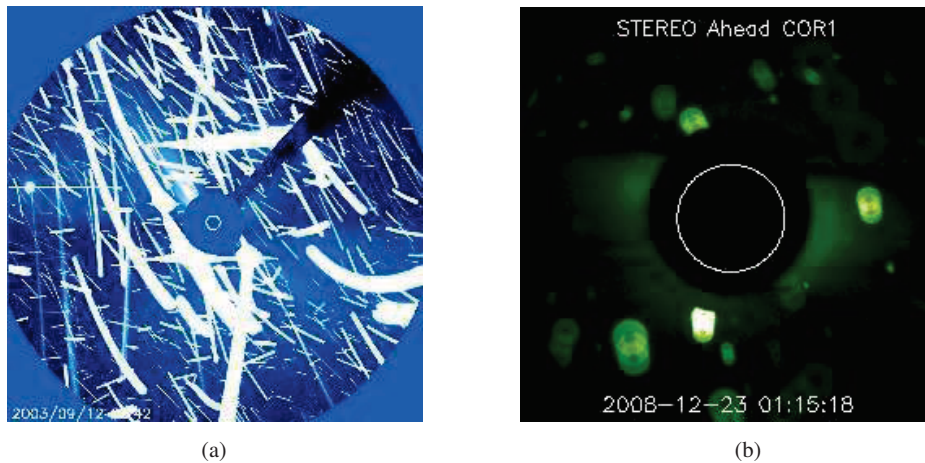


Figure 5 Example of bright blobs and streaks acquired with coronagraphs. (a) Image taken by the LASCO C3 coronagraph on 12 September 2003 [12] (b) Debris event observed by the STEREO Ahead COR1 telescope on December 23, 2008 [11].

The small debris particles are brightly illuminated by the Sun, and are easily seen by the coronagraphs if they wander into their field of views. This is similar to the effect of a sunbeam shining through a window and scattering from the minute dust particles suspended in the air.

Since the instruments are focused at infinity, but the particles are in general quite close to the instrument aperture, the acquired images are often tremendously out-of-focus. For example, in the COR1 and COR2 telescopes because of the central occulter in these telescopes, the images often appear as "donut" shapes (see Figure 5b). The bigger the particle image appears, the closer it is to the telescope. Assuming that the particle is otherwise very small, the image size can be used to determine how far away the particle is from the instrument.

Since the particles are moving with respect to the spacecraft, the length of the streak depends upon how fast the particle is moving, and how far it is from the instrument. For a given speed, the closer the particle is, the longer the track.

If the acquired frames are built up from a series of images, taken some minutes apart one from the other and then averaged, the same particle will often show up multiple times in the same frame. If some frames are taken in succession one after the other, the track of the particle in one frame can continue in the subsequent frame.

3.2 Images of the out-of-focus spots in the FoV

To understand the Metis out-of-focus images formation and appearance, we decided to perform some simulations with the Zemax raytracing code using the visible light channel model.

As discussed in section 2, the Metis optical design is quite peculiar. The pupil of the instrument is only partially filled with light; the M0 mirror and the IO and FS are vignetting the beam. Even at the edges of the FoV, only about half of the pupil is usefully illuminated. See Figure 6 for a clear visualization of the phenomenon; the pupil and its light filling in function of the FoV are depicted. Starting from the inner FoV region, the illuminated area is a sort of crescent moon, but it never becomes a “full moon”; at the edges of the field of view it is about a “first quarter moon”. This fact is also reflected in the vignetting function, see Figure 3b, where the value of the unvignetted rays fraction, even at the edges of the FoV, is always less than 50%.

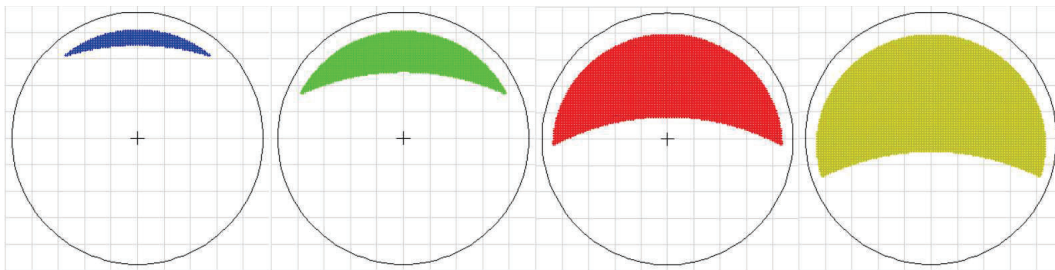


Figure 6. The Entrance Pupil (IEO) circular aperture, 40 mm in diameter, and its light filling with respect to the FoV. The represented fields from the left are 1.7°, 2.0°, 2.5° and 2.9° with a fraction of unvignetted rays respectively of 3, 12, 31 and 46%. The fields are taken along the central line of the detector to avoid the region affected by the spiders.

For creating Figure 6, the field angles have been chosen, on purpose, to be placed on the y direction (see Figure 1 for the reference system definition), to avoid the region along the diagonals affected by the spiders. As stated in the section 2.2, the spiders used to mount the IEO/FS assembly and M0/FS are furtherly vignetting the beam. If a direction in the field oriented at 45° is considered, the shapes of the rays in the pupil are as shown in Figure 7. The shadow due to the spider is clearly visible; it is located exactly in the center of the images, since we have considered field angles perfectly located along the diagonal, if we were to consider other positions the shadow would be decentered.

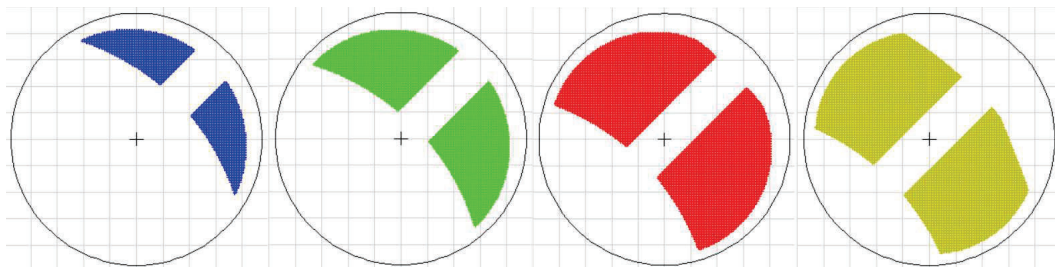


Figure 7. The Entrance Pupil (IEO) circular aperture, 40 mm in diameter, and its light filling with respect to the FoV along the spider at 45° inclination. The represented field angles, starting from the left, are 2.1°, 2.5°, 3.1° and 3.4° with a fraction of unvignetted rays respectively of 12, 25, 42 and 42%.

Considering some out-of-focus sources in the FoV, it is possible to simulate the appearance of their images on the detector. Taking a point source at a distance of 2 meters from the Metis entrance aperture and placing it in different positions in the FoV, the footprint spot diagrams in Figure 8 can be derived. The out-of-focus images are very much like the pupil filling patterns previously seen. Considering the sources placed along the x and y direction, corresponding to the rows and columns of the detector, the ‘crescent moon’ pattern is clearly visible (see Figure 8 a and b). Considering the point sources

placed along the system diagonals, the images are still ‘crescent moon’ like but they are divided in two parts by the shadow of the spiders. If the point sources are not exactly along the diagonal, their images are still divided in two pieces by the spider shadow, but the pieces will have different sizes depending on how far the considered point source is from the diagonal (see Figure 8 c and d).

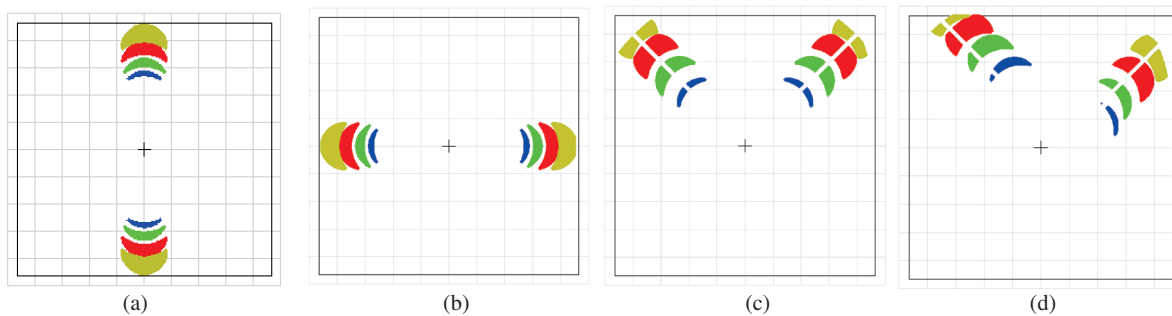


Figure 8. Simulated out-of-focus spot images for eight sources positioned in different points in the FoV. In (a) and (b) the sources have been placed in different points corresponding to the direction of the x and y axes of the detector. In (c) and (d), the sources have been placed almost along the detector diagonals to highlight the effect of the spiders shadow. The external square represents the VL detector (20.48x20.48 mm²).

Moving further with the simulation, random points in the FoV can be considered see Figure 9. In (a) there is a footprint diagram, different image points, affected or not by the spiders shadow, are visible. In (b) there is a much realistic simulation using the ‘‘image simulation’’ feature of Zemax and applying the black and white color visualization. Point sources in (a) and (b) are located at 1 meter from the entrance aperture of the coronagraph. The point source number and distribution are not exactly the same for (a) and (b). In (b) and (c) the point source distribution is the same, but for (c) the sources have been placed at 2 m from IEO. All the images have been simulated and displayed considering the VL detector dimensions, i.e. 2k x 2k, pixel size 10 μm , 20.48 mm x 20.48 mm.

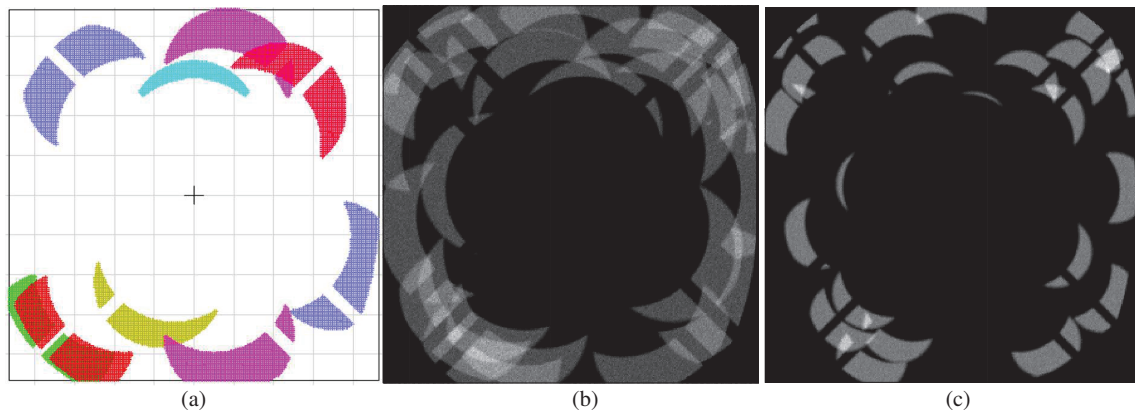


Figure 9. Simulated image with point sources place in different points inside the FoV. In (a) simulated as ‘footprint diagram’ in (b) in black and white to be more similar to the acquired Metis images. In (a) and (b) the sources are placed at 1 m from the entrance aperture in (c) at 2 m.

The dimensions of the out-of-focus spots are obviously directly related with the distance. Comparing Figure 9 b and c the difference in the dimension of the spots is clearly visible. As a rule of thumb, considering the pupil fully illuminated, the dimension of the image of an out-of-focus point source is related with the distance via the formula $f D/p$, where f is the focal length, D the diameter of the entrance pupil, and p the distance of the source. For Metis $f D$ is 8 m*mm, so for particles at 1 m distance the dimension of the out-of-focus image is of the order of 8 mm, while for a distance of 2 m the size is 4 mm and so on.

Trying to perform an even more realistic simulation, sources with different intensities and sizes have been considered, see Figure 10. In this figure, a particle distribution represented in (a) has been considered to be placed at 5, 2, and 1 m from the entrance aperture. The different intensity of the sources is clear visible as the corresponding images have different

intensity. The difference in the extension of the source is also clearly visible in the images since the out-of-focus images appear to be less sharp being the result of the superimposition of many “just a little shifted” images.

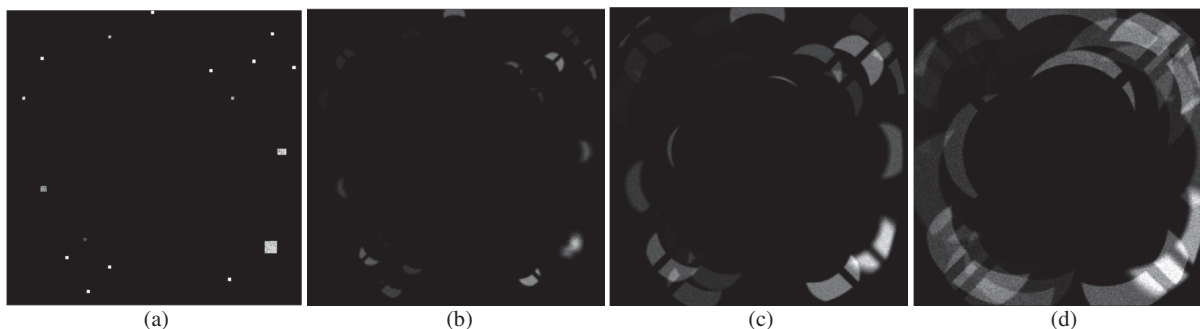


Figure 10. Simulated images with the sources with different intensity and sizes inside the FoV. The sources have been placed at different points inside the FoV and with different distances from Metis. In (a) the sources have been placed at infinity, in (b) (c) and (d) respectively at 5, 2 and 1 meter from the Metis IEO aperture.

The next step in the simulation process is to try to replicate a moving particle. The point sources have been simulated to move in different directions in the FoV of Metis, see Figure 11a for the simulated input tracks. This ‘moving particle’ pattern has been placed at 5, 2 and 1 m from the entrance aperture of Metis and the correspondent image simulations are reported in Figure 11(b), (c), and (d) respectively. It can be seen that the thickness of the image tracks are obviously related with the distance. As for the tracks passing through the area affected by the spiders, the corresponding shadows are visible. It has to be highlighted that, due to the motion of the particles, the shadow could be seen also moving and generating black tracks that are no more parallel to the real inclination of the spiders but are following the direction of the track of the particle itself.

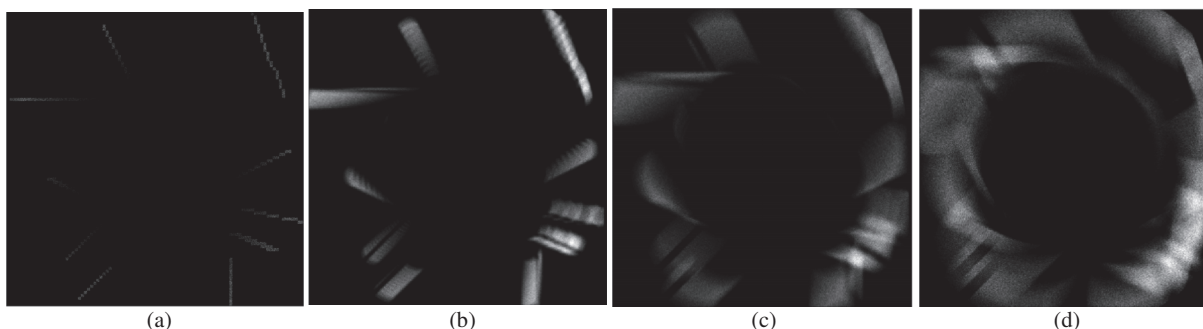


Figure 11. Simulated images with the sources moving inside the FoV. The sources have been placed at different points inside the FoV and with different distances from Metis. In (a) the sources have been placed at infinity, in (b) (c) and (d) respectively at 5, 2 and 1 meter from the Metis IEO aperture.

Coming back to the images acquired by Metis, many of the features we have discussed in the simulations can be seen. In particular, the shadows of the spiders are visible in many blobs and not always inclined with the same angle, indicating the particle has moved during the acquisition in that specific direction. The blobs are of different sizes depending on their distance from the instrument. The effects are further visible if different successive images are summed together as in Figure 12, where three 5 s exposure time images have been combined.

In Figure 13 a single particle event registered over three consecutive 5 s exposure time images has been displayed and the corresponding raytracing simulation has been performed to visually compare the result. The edges of the tracks are larger and with the shadow of the spiders clearly visible while the center is thinner. This peculiar pattern is due to the changing shape of the out-of-focus image along the track as visualized, not to scale, in Figure 14.

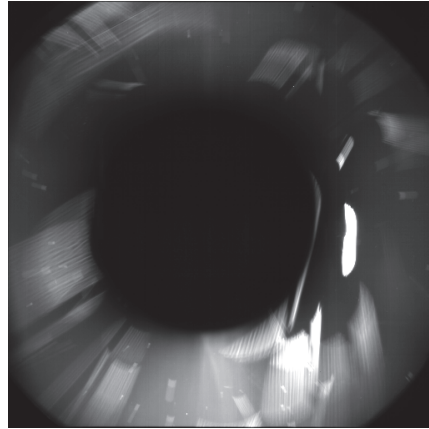


Figure 12. Combination of three successive Metis images acquired during the June ‘particle’ event.

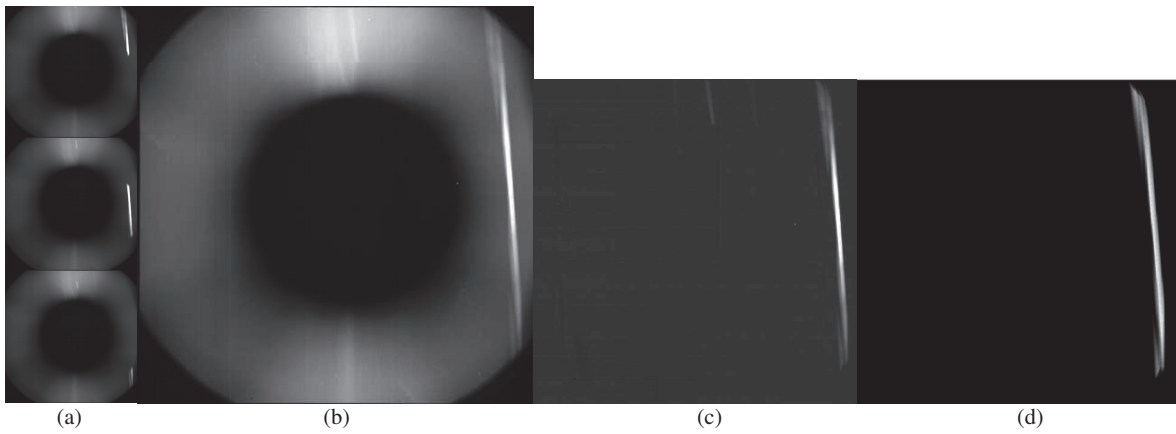


Figure 13. Example of a particle passage in the Metis FoV. Three successive images (a), their sum (b) the particle track with the solar corona removed (c) and the raytracing simulation (d).

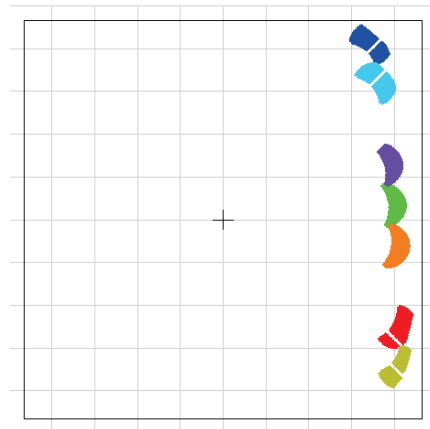


Figure 14. Visual explanation of the pattern of the track formation. Examples of the out-of-focus point source image evolution through the track are shown. The dimension of the images has been exaggerated to clearly show the phenomenon.

4. CONCLUSIONS

From time to time, the Metis coronagraph onboard the Solar Orbiter ESA/NASA mission is imaging blobs and streaks likely to be generated by particles passing near the instrument and traversing the Metis FoV. Some simulations with the Zemax raytracing software have been done in order to study the peculiar pattern these out-of-focus images exhibit.

Starting from the description of the vignetting function, the shape and size of the out-of-focus images have been studied taking also into account their variation with the distance of the sources from the Metis telescope entrance aperture. The patterns seen in the Metis images acquired during the commissioning in June 2020, when one of these events happened, have been discussed and are in accordance with the simulation results.

ACKNOWLEDGMENTS

The Metis program is supported by the Italian Space Agency (ASI) under the contracts to the co-financing National Institute of Astrophysics (INAF): Accordi ASI-INAF N. I-043-10-0 and Addendum N. I-013-12-0/1, Accordo ASI-INAF N. 2018-30-HH.0 and under the contracts to the industrial partners: ASI-TASI N. I-037-11-0 and ASI-ATI N. 2013-057-I.0. The Metis team thanks Barbara Negri, Enrico Flamini, Marco Castronuovo of the Italian Space Agency and Roberto Della Ceca, Giuseppe Malaguti of the Istituto Nazionale di Astrofisica for their continuous support during the development of the coronagraph. A special thanks to Filippo Marliani of the European Space Agency for his dedication to the program and his high standard of excellence. The testing of Metis was performed by an industrial consortium constituted by OHB Italia S.p.A. (acting as Prime Contractor towards ASI), Thales Alenia Space Italia S.p.A. (Co-Prime Contractor with the specific responsibility of the instrument AIT). ALTEC has provided logistics and technical support for the INAF Optical Payload Systems. The primary and secondary mirrors were provided as a Czech contribution to Metis; the mirror hardware development was possible thanks to the Czech PRODEX Programme. The UVDA assembly was provided as a German contribution to Metis, thanks to the financial support of DLR (grant 50 OT 1201). The VLDA assembly was provided under Contract 2013-058-I.0 with the Italian Space Agency (ASI). The Metis team thanks the former PI, Ester Antonucci, for leading the development of Metis until the final delivery to ESA.

REFERENCES

- [1] Muller, D., St. Cyr, O. C., Zouganelis, I., Gilbert, H. R., Marsden, R., Nieves-Chinchilla, T., Antonucci, E., Auchere, F., Berghmans, D., Horbury, T. S., Howard, R. A., Krucker, S., Maksimovic, M., Owen, C. J., Rochus, P., Rodriguez-Pacheco, J., Romoli, M., Solanki, S. K., Bruno, R., Carlsson, M., Fludra, A., Harra, L., Hassler, D. M., Livi, S., Louarn, P., Peter, H., Schühle, U., Teriaca, L., del Toro Iniesta, J. C., Wimmer-Schweingruber, R. F., Marsch, E., Velli, M., De Groof, A., Walsh, A., and Williams, D., "The Solar Orbiter mission. Science overview," *642*, A1 (Oct. 2020).
- [2] Antonucci, E. et al., "Metis: the Solar Orbiter visible light and ultraviolet coronal imager," *A&A* **642**, A10 (2020).
- [3] Romoli, M., et al., "Challenges during Metis-Solar Orbiter commissioning phase", Proc. SPIE 11852, International Conference on Space Optics-ICSO 2020, 118525A (2021).
- [4] Romoli, M., Landini, F., Antonucci, E., Andretta, V., Berlicki, A., Fineschi, S., Moses, J. D., Naletto, G., Nicolosi, P., Nicolini, G., Spadaro, D., Teriaca, L., Baccani, C., Focardi, M., Pancrazzi, M., Pucci, S., Abbo, L., Bemporad, A., Capobianco, G., Massone, G., Telloni, D., Magli, E., Da Deppo, V., Frassetto, F., Pelizzo, M. G., Poletto, L., Uslenghi, M., Vives, S., Malvezzi, M., "METIS: the visible and UV coronagraph for solar orbiter," Proc. SPIE 10563, 105631M (2017).
- [5] Fineschi, S. et al., "Optical design of the multi-wavelength imaging coronagraph Metis for the solar orbiter mission," *Exp. Astron.* **49**, 239-263 (2020).
- [6] Da Deppo, V., et al., "Alignment procedure for the Gregorian telescope of the Metis coronagraph for the Solar Orbiter ESA mission," Proc. SPIE 11180, International Conference on Space Optics — ICSO 2018, 1118076 (2019).
- [7] Sandri, P., et al., "Stray-light analyses of the multielement telescope for imaging and spectroscopy coronagraph Solar orbiter," *Opt. Eng.* **57**(1), 015108 (2018).
- [8] Landini, F., et al., "In flight stray light reduction for the Solar Orbiter/Metis coronagraph", International Conference on Space Optics 2022, to be published in Proc. SPIE, this volume (2022).

- [9] Casini, C., et al., “Theoretical, on-ground and in-flight study of the Metis coronagraph vignetting”, in International Conference on Space Optics 2022-ICSO 2022, to be published in Proc. SPIE, this volume (2022).
- [10] Liberatore, A., et al., “In-flight calibration of Metis coronagraph on board of Solar Orbiter”, Proc. SPIE 11852, International Conference on Space Optics-ICSO 2020, 1185248 (2021).
- [11] https://stereo.gsfc.nasa.gov/artifacts/artifacts_debris.shtml
- [12] <https://soho.nascom.nasa.gov/pickoftheweek/old/17sep2003/index.html>
- [13] <https://lasco-www.nrl.navy.mil/index.php?p=content/debris>